7-2019

The mechanical behavior of brain surrogates manufactured from silicone elastomers

Ling Zhang
Iowa State University, lingz@iastate.edu

William J. Jackson
Iowa State University, wjack@iastate.edu

Sarah A. Bentil
Iowa State University, sbentil@iastate.edu

The mechanical behavior of brain surrogates manufactured from silicone elastomers

Abstract
The ongoing conflict against terrorism has resulted in an escalation of blast-induced traumatic brain injuries (bTBI) caused by improvised explosive devices (IEDs). The destructive IEDs create a blast wave that travels through the atmosphere. Blast-induced traumatic brain injuries, attributed to the blast wave, can cause life-threatening injuries and fatalities. This study aims to find a surrogate brain material for assessing the effectiveness of head protection systems designed to mitigate bTBI. Polydimethylsiloxane (PDMS) is considered as the surrogate brain material. The stiffness of PDMS (Sylgard 184, Dow Corning Corp.) can be controlled by varying the ratio of base and curing agent. Cylindrical PDMS specimen with ratios of 1:10, 1:70, and 1:80 were subjected to unconfined compression experiments at linear rates of 5 mm/min, 50 mm/min, and 500 mm/min. A ramp-hold strain profile was used to simulate a stress relaxation experiment. The fractional Zener viscoelastic model was used to describe the stress relaxation response, after optimization of the material constants for the brain surrogate and shock wave exposure brain tissue. The results show that the low cost PDMS can be used as a surrogate brain material to study the dynamic brain response to blast wave exposure.

Keywords
TBI, Polydimethylsiloxane, PDMS, Brain surrogate, Brain simulant, Fractional zener

Disciplines
Biology and Biomimetic Materials | Biomechanical Engineering | Polymer and Organic Materials

Comments
This is a manuscript of an article published as Zhang, Ling, William J. Jackson, and Sarah A. Bentil. "The mechanical behavior of brain surrogates manufactured from silicone elastomers." *Journal of the Mechanical Behavior of Biomedical Materials* 95 (2019): 180-190. DOI: 10.1016/j.jmbbm.2019.04.005. Posted with permission.

The Mechanical Behavior of Brain Surrogates Manufactured from Silicone Elastomers

Ling Zhang[a], William J. Jackson[a], Sarah A. Bentil[a,*]

[a]*Department of Mechanical Engineering, Iowa State University of Science and Technology, 2529 Union Drive, Ames, IA 50011, USA*

Abstract

The ongoing conflict against terrorism has resulted in an escalation of blast-induced traumatic brain injuries (bTBI) caused by improvised explosive devices (IEDs). The destructive IEDs create a blast wave that travels through the atmosphere. Blast-induced traumatic brain injuries, attributed to the blast wave, can cause life-threatening injuries and fatalities. This study aims to find a surrogate brain material for assessing the effectiveness of head protection systems designed to mitigate bTBI. Polydimethylsiloxane (PDMS) is considered as the surrogate brain material. The stiffness of PDMS (Sylgard 184, Dow Corning Corp.) can be controlled by varying the ratio of base and curing agent. Cylindrical PDMS specimen with ratios of 1:10, 1:70, and 1:80 were subjected to unconfined compression experiments at linear rates of 5 mm/min, 50 mm/min, and 500 mm/min. A ramp-hold strain profile was used to simulate a stress relaxation experiment. The fractional Zener viscoelastic model was used to describe the stress relaxation response, after optimization of the material constants for the brain surrogate and shock wave exposure brain tissue. The results show that the low cost PDMS can be used as a surrogate brain material to study the dynamic brain response to blast wave exposure.

Keywords:
TBI, Polydimethylsiloxane; PDMS; Brain surrogate; Brain simulant; fractional Zener

*Corresponding author:
Email address: sbentil@iastate.edu (Sarah A. Bentil)
URL: www.me.iastate.edu/sbentil/ (Sarah A. Bentil)

1. Introduction

Improvised explosive devices (IEDs), used during the war against terrorism, have caused blast-related injuries and coalition deaths. Detonation of the IEDs result in a shock wave that causes an increase in overpressure. The shock wave travels through the atmosphere. When the shock wave propagates through the head of an individual, the brain can be injured by the overpressure (Nakagawa et al., 2011). This injury is classified as primary blast-induced traumatic brain injury (bTBI). The mechanism of bTBI is still not well understood (Ghajari et al., 2017; Gu et al., 2017; Iwaskiw et al., 2018). We aim to apply the mechanical response of brain tissue that have and have not been exposed to a shock wave, as a means of designing a surrogate brain for future bTBI mechanism studies. Considering the difficulties involved in obtaining and conducting experiments on human and animal brain tissue to understand mechanisms of injury and characterize the mechanical response, the availability of a viable brain tissue surrogate would be beneficial.

Soft polymeric materials have been used to simulate brain tissue in many applications. For example, Chanda et al. (2016) fabricated a two-part silicone-based material system to simulate gray and white matter for human brain tissue surrogate. Tension test of specimens has been conducted by Chanda et al. (2016) at linear rate 2.5 mm/s and 30 mm/s. They found that the mechanical behavior of brain tissues at two different strain rates can be characterized with two different two-part silicone compositions (Chanda et al., 2016). Ploch et al. (2016) considered ballistic gelatin as a material for three-dimensional (3D) printing of brain models. These brain models were used for Neurosurgical Training and Preoperative Planning. Hossain (2010) used gelatin and silicone gels as the surrogate brain material for a Realistic Explosive Dummy Head (RED Head). This head model was used to perform blast loading experiments in laboratory to understand the blast loading injury mechanics. Alley et al. (2011) conducted blast tests with spherical poly (methyl methacrylate) (PMMA) shells that were filled with a brain surrogate fabricated with Perma-Gel^{TM} ballistic gelatin and polydimethylsiloxane (PDMS) silicone elastomer. Mediavilla Varas et al. (2011) also utilized a spherical skull, but considered a gelatinous brain surrogate. The skull-brain system was placed inside a square shock tube to study the mechanisms of blast-induced mild traumatic brain injury.

Water and oil have also been considered as a brain surrogate, and have

been used to fill the interior of a skull surrogate material. Hua et al. (2014) have used a water-filled polycarbonate shell to study blast injury. In 2013, Selvan et al. (2013) filled a cylinder with mineral oil and subjected the device to blast load. Mineral oil was used instead of water to reduce cavitation effects (Selvan et al., 2013). However, brains have different material properties than fluids, and exhibit a non-linear and strain rate behavior when subjected to external loads (Schiavone et al., 2009).

To compare the mechanical response of soft materials and brain tissue, rheological tests have been conducted. Hossain (2010) has performed step response analysis, rheometry analysis, and dynamic mechanical analysis (DMA) of materials that include gelatin, toothpaste, custard powder, and silicone gels. The aforementioned materials were compared with brain tissue. From the study by Hossain (2010), the gelatins and silicone gels produced a mechanical response that closely mimicked brain tissue. Moreover, from the study by Alley et al. (2011), they found that a brain surrogate fabricated with Perma-Gel^{TM} ballistic gelatin was stiffer and less viscous when compared with the PDMS silicone elastomer.

The literature has shown that PDMS is a suitable choice for a brain surrogate (Alley et al., 2011; Hossain, 2010). However, the material properties of PDMS that is comparable to the brain is unknown. For decades, constitutive models have been developed for soft materials and tissues to obtain the material properties (Miller and Chinzei, 2002; Lu et al., 2016; Qi and Boyce, 2004; Sollich, 1998; Miller, 1999). In 1996, a viscoelastic constitutive model was developed for high-polymeric materials under varying temperature (Holzapfel and Simo, 1996). Another viscoelastic model, using concepts from nonlinear constitutive theory, has been developed for fiber-reinforced composite materials (Holzapfel and Gasser, 2001). Takagi et al. (2008) developed a model for polymer deformation during the thermal imprint process using the generalized Maxwell model.

A nonlinear viscoelastic model was developed, using the Zener model, to describe the mechanical responses of a semi-crystalline polymer subjected to isothermal deformation at small strains (Lai et al., 2005). The fractional Zener (FZ) viscoelastic model has also been applied in the literature to characterize the response of the brain to mechanical loads (Davis et al., 2006; Kohandel et al., 2005; Carmichael et al., 2015; Bentil and Dupaix, 2014, 2018). Kohandel et al. (2005) used the fractional Zener model to describe the dynamic behavior of brain tissue. They fitted the model to experimental data of bovine brain tissue subjected to oscillatory shear, to obtain the

constitutive model parameters of the soft tissue. In 2014, Bentil and Dupaix (2014) used the fractional Zener model to describe the mechanical behavior of compressed brain tissues subjected to low strain rates. A ramp-hold strain input was applied in compression tests of pig brain tissue, to simulate a stress relaxation test. The hold corresponded to a constant strain application on the brain. Bentil and Dupaix (2014) demonstrated that the fractional Zener model provides a better fit for the experimental data than the Zener model, due to the ability to capture the response from both the ramp and hold input. In this study, we apply the fractional Zener constitutive model to characterize and compare the mechanical response of PDMS and brain tissue. Brain tissue exposed and unexposed to a shock wave is used in the comparison.

2. Method and Material

2.1. Preparation of PDMS as a Brain Surrogate

For years, soft materials have been studied to simulate tissue such as skin, liver, lung, and brain. Gelatin and polydimethylsiloxane are materials commonly used for skin surrogates (Chanda, 2018; Payne et al., 2015) and brain tissue surrogate (Alley et al., 2011; Ploch et al., 2016). Polydimethylsiloxane (Sylgard 184, Dow Corning Corporation) is a silicon-based crosslinked polymer. Sylgard 184 is made by mixing a two-part liquid component kit containing a curing agent (or part B) and base (or part A). The suggested ratio for Sylgard 184 is 1:10 (curing agent / base) by weight or volume (Corning, 2018). By varying the ratio, Sylgard 184 can be fabricated with different stiffnesses. In 2007, PDMS of ratios ranging from 1:30 to 1:60 were fabricated; however, a ratio of 1:70 or above caused the silicone elastomer to remain as a highly viscous liquid (Supplementary Material (ESI) for Lab on a Chip, 2007). In 2010, Miquelard-Garnier et al. (2010) measured the Young's modulus of PDMS substrates of ratios between 1:20 and 1:40. The range of Young's modulus was between 120 kPa and 750 kPa, with the stiffer modulus corresponding to the smaller ratio (Miquelard-Garnier et al., 2010). Wang et al. (2014) fabricated PDMS with ratios ranging from 1:5 to 1:33. By testing the PDMS samples under compression, the elastic modulus ranged from 0.56 MPa to 3.59 MPa. In comparison, the Young's modulus of brain tissue ranges between 10 – 30 kPa (Masoumi et al., 2013). PDMS with a ratio of 1:60 is still stiffer than brain tissue. To simulate brain tissue using a silicone elastomer, a higher ratio of curing agent to base is needed.

Since PDMS is a polymer that can be cured by heat, a ratio of 1:80 can be fabricated by increasing the curing temperature.

Sylgard 184 PDMS kit was used to produce cylindrical brain surrogate samples. The curing agent and base were weighed using a PA 163 Electronic Balance (Ohaus Corporation). Titanium dioxide (TiO_2) powder was added to produce an opaque white specimen instead of a transparent specimen (Bentil et al., 2016). The mass of the powder is 0.04 – 0.1 g, which is approximately 0.1% of the total mass of PDMS. The base, curing agent, and titanium dioxide powder were mixed for 20 minutes. The mixture was poured into a cylindrical steel mold, which has a 25 mm inner diameter. The steel mold was utilized to facilitate curing of PDMS at increased curing temperatures. After mixing, the solution was degassed in a vacuum for 1 hour (Bentil et al., 2016). The specimen was then cured by incubating for 1 hour to 2 days at 100 – 110°C. Following the incubation period, the specimen was left in the mold at room temperature for at least one day. The specimen was then removed from the mold.

The ratio of curing agent and base ranges in this work are 1:10, 1:70, and 1:80. Detailed information of the PDMS samples prepared are shown in table 1. All cylindrical PDMS samples were subjected to unconfined compression stress relaxation experiments with a linear rate of 5 mm/min, 50 mm/min, and 500 mm/min. Samples were compressed to 20% strain to characterize the mechanical behavior.

Table 1: Details of the PDMS Samples.

PDMS Sample	Height (mm)	Error of ratio (%)	Curing time
PDMS 1:10	18.2	0.08	1 hour
PDMS 1:70	18.4	0.02	2 days
PDMS 1:80	18.5	1.10	2 days

2.2. Preparation of Pig Brain for Shock wave Exposure

To study blast-induced traumatic brain injury mechanisms, small animals like rats (Clemedson et al., 1953; Clemedson and Hultman, 1954; Clemedson, 1956) have commonly been used due to availability. Pigs have been used to study brain activity during and after a blast wave exposure (Bauman et al., 2009; Axelsson et al., 2000). In this work, a pig brain is used to simulate

human brain since the vascular system and the gyri and sulci are anatomically similar with a human brain (Säljö et al., 2008). Pig heads were obtained from Iowa State University's abattoir and the whole brains were extracted and tested within 6 – 8 hours after animal sacrifice. The average mass of the pig brain was 85.8 g.

The extracted pig brains were tested within 10 minutes, at room temperature (20°C). The test consisted of shock wave exposure for pig brains, followed by unconfined compression experiments. Brain tissue without shock wave exposure, served as the control, and was also subjected to unconfined compression experiments.

An air pistol (.177 caliber Crosman Pumpmaster Classic) was utilized to create the shock wave, as a means of simulating the blast exposure (Courtney et al., 2015). The air pistol did not contain any pellets and served as the driver. This driver is connected to a 64-cm long Schedule 40 polyvinyl chloride (PVC) pipe (driven section), with a nominal size of 1/2 in. (12.7 mm). The shock wave was traveling at Mach 1.3. The pig brain is adhered to a block at the end of the pipe using glue. The distance between the end of the pipe and the pig brain is 5 mm. Figure 1 is a schematic of the experimental setup for pig brains exposed to shock waves. The experimental setup described in figure 1 was fixed on the top surface of an optical table. The shock wave was generated by pumping the air pistol 10 times, before releasing the compressed air. Releasing the compressed air created a shock front that propagated through the pipe and impacted the pig brain. The reflected shock wave pressure after 10 pumps was 103.5 kPa – 124.2 kPa (15 – 18 psig), which was measured using a pressure transducer (PCB 113B24). The pressure transducer is placed 5 mm away from the end of the pipe. Figure 2 shows the reflected shock wave's pressure–time history measured by the pressure transducer. Each pig brain was exposed to the shock wave five times, on either the left or right hemisphere (near the temporal lobe), to increase the simulated primary bTBI effect. A preliminary study in the lab showed that brain's exposed to a single shock wave produced a stress response with a comparable magnitude as brain's that were not exposed to a shock wave, when subjected to unconfined compression tests. A difference in the stress response magnitude is observed after brain's are exposed to a shock wave five times.

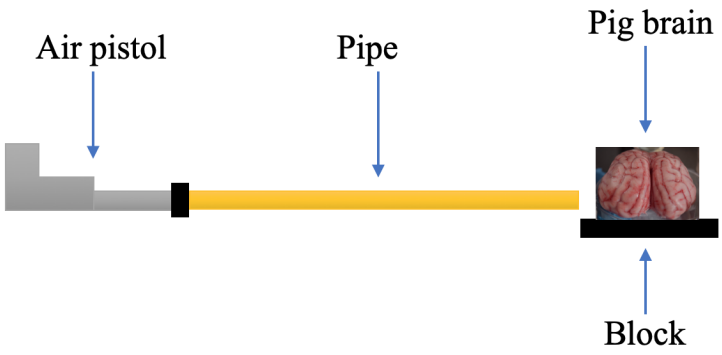

Figure 1: Experimental setup for pig brains exposed to shock wave (side view).

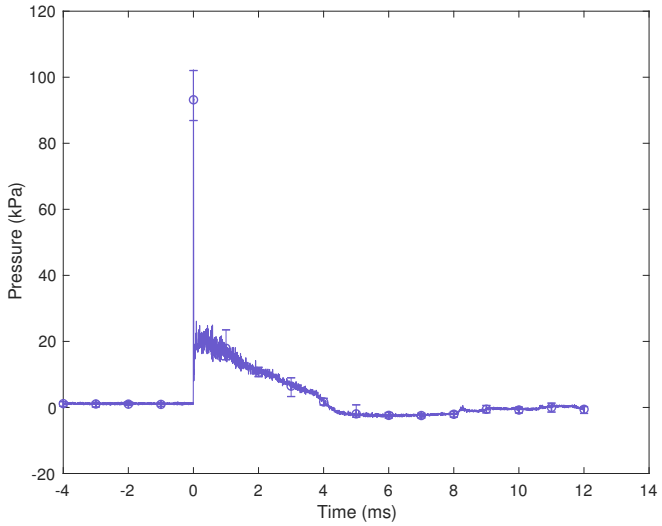

Figure 2: Pressure–time history of the reflected shock wave, measured 5 mm away from the end of the pipe. Error bars denote standard deviation following 10 runs at the aforementioned location.

2.3. Unconfined Compression Test using the HR-2 Rheometer

Unconfined compression tests were conducted with a Discovery Hybrid Rheometer (HR-2, TA Instruments), as shown in figure 3, to investigate the mechanical response of PDMS and pig brain. Brain's exposed to a shock wave were tested using the HR-2 within 5 – 10 minutes, to minimize variation in the tissue response from dehydration.

Figure 3: Cylindrical PDMS specimen (white) during unconfined compression experiments with the HR-2 rheometer. A ramp-hold loading rate was applied to obtain the stress relaxation response of PDMS and pig brain tissue.

Prior to the unconfined compression test, a 25-mm-diameter coring tool was used to core pig brain samples into a cylindrical shape. The average height of the cored brain is 15.9 mm. The deviation of the height is up to 38% due to cutting some brain samples in the plane parallel to the cylinder's bottom, to ensure that the sample remained upright during the unconfined compression experiments. Cored brain tissue, consisting of both gray and white matter, was obtained from both the left and right hemisphere. Additional details of the pig brain samples is shown in table 2.

A ramp-hold loading rate was applied on PDMS and pig brain samples. The first step is ramp, where the brain sample was compressed to 20% strain at a linear rate of either 5 mm/min, 50 mm/min, and 500 mm/min. As the linear rate increased to 500 mm/min, the brain sample was compressed to a strain of 5%, due to the limitation of the HR-2. Once the ramp step is completed, the hold phase begins. During the hold step, the brain is held at the desired strain for a duration of two minutes. A preload of 0.01 – 0.04 N was applied to ensure that the top and bottom surface of the sample were in contact for each test. The same HR-2 protocol was applied for the cylindrical PDMS samples of different ratios, which were also prepared with the same diameter as the pig brain. Figure 3 shows a PDMS sample tested on the HR-2.

Table 2: Details of the Pig Brain Samples (SWE: Shock Wave Exposure; NSWE: No Shock Wave Exposure).

Number of Pig Brain Samples	Shock Wave Exposure Condition	Strain Rate (mm/min)	Averaged Mass of Brain (g)	Averaged Core Height (mm)
3	SWE	5	83.9	16.2
3	SWE	50	88.3	16.2
4	SWE	500	83.3	12.0
2	NSWE	5	86.3	17.7
2	NSWE	50	84.2	17.6
4	NSWE	500	90.1	12.4

2.4. Curve fit by using Fractional Zener Constitutive Model

The fractional Zener model contains a fractional order 'spring-pot' element (i.e. fractional element) that has been used to describe viscoelastic response in creep (Xu and Jiang, 2017) and relaxation experiments (Bentil and Dupaix, 2014, 2018; Davis et al., 2006). The fractional element was developed by Scott-Blair in 1947 (Xu and Jiang, 2017; Mainardi, 2010). Equations 1, 2, and 3 (Bentil and Dupaix, 2014; Craiem and Magin, 2010) show the stress-strain relations for the fractional, spring, and spring-pot (or dashpot) elements, respectively. For the fractional element, α is between 0 and 1, which implies that the viscoelastic material is on a spectrum that ranges between an elastic solid ($\alpha = 0$) and Newtonian fluid ($\alpha = 1$) (Bentil and Dupaix, 2014).

$$\sigma(t) = E\tau^{\alpha} D^{\alpha}\varepsilon(t),\ 0 < \alpha < 1 \tag{1}$$

$$\sigma(t) = E\varepsilon(t),\ \alpha = 0 \tag{2}$$

$$\sigma(t) = E\tau D\varepsilon(t) = \eta\varepsilon(t),\ \alpha = 1 \tag{3}$$

In equations 1 – 3, E is the elastic property, η is the viscosity of the material, τ is the relaxation time, and D is the differintegral operator (Bentil and Dupaix, 2014; Craiem and Magin, 2010).

The fractional Zener constitutive model is a combination of two springs and a spring-pot (Bentil and Dupaix, 2014). Solving the rheological system,

the stress-strain relation is shown in Eq. 4 (Bentil and Dupaix, 2014). The four parameters in Eq. 4 that need to be optimized by using the brain tissue and PDMS experiment data are: E_∞, E_0, τ_0, and α.

$$\sigma(t) + \tau_0^\alpha D^\alpha \sigma(t) = E_\infty \varepsilon(t) + E_0 \tau_0^\alpha D^\alpha \varepsilon(t),\ 0 < \alpha < 1 \tag{4}$$

where E_0 is the brain's instantaneous modulus or initial elastic response, E_∞ is the long-term stiffness, τ_0, is the relaxation time, and α gives a sense of the brain material's location on the viscoelastic spectrum (Bentil and Dupaix, 2014).

2.5. Statistical Analysis

A hierarchial statistical approach was applied to analyze the data. First, an analysis of variance (ANOVA) study is conducted, using the statistical software JMP (JMP, 2015), to identify the most sensitive factors (i.e. 'All Samples' and 'Compression Rate') that will affect the FZ coefficients and also the maximum engineering stress (σ_{max}). The factor 'All Samples' has four levels: Pig brain NSWE, Pig brain SWE, PDMS 1:70, and PDMS 1:80. Both PDMS 1:70 and PDMS 1:80 were not exposed to a shock wave (NSWE condition), since the aim of this work is to determine which PDMS ratio will mimic the response of SWE and NSWE brains. The factor 'Compression Rate' has three levels: 5 mm/min, 50 mm/min, and 500 mm/min. A discrete factor effects model was used to test the factors, and its binary interaction, at a significance level of 0.05. Then, a pairwise comparison of a factor's levels are made using a Tukey Honestly Significant Difference (HSD) test, as appropriate, at a significance level of 0.05.

3. Results

3.1. Unconfined Compression Test using the HR-2 Rheometer

Stress relaxation experiments were conducted on brain tissue and PDMS samples. Figure 4 shows the ramp-hold strain profile for the stress relaxation experiments. The ramp phase describes linear compression of the sample to a desired strain. The hold phase immediately follows the ramp phase, and consists of the sample relaxing at the desired strain for two minutes. As is shown by figure 4, at low linear rates (5 mm/min and 50 mm/min), the desired strain applied on the sample was 20%. The deviation of strain from the desired magnitude is higher for pig brain samples than PDMS. For the

high linear rate of 500 mm/min, the sample strain reached was 5%, even though the desired strain value was 20%. This was due to limitations of the HR-2 rheometer preventing samples compressed at 500 mm/min from reaching a desired strain of 20%. Although the results can not be compared between the high and low linear rates, due to the varying strains reached, the strain remained consistent for each linear rate considered.

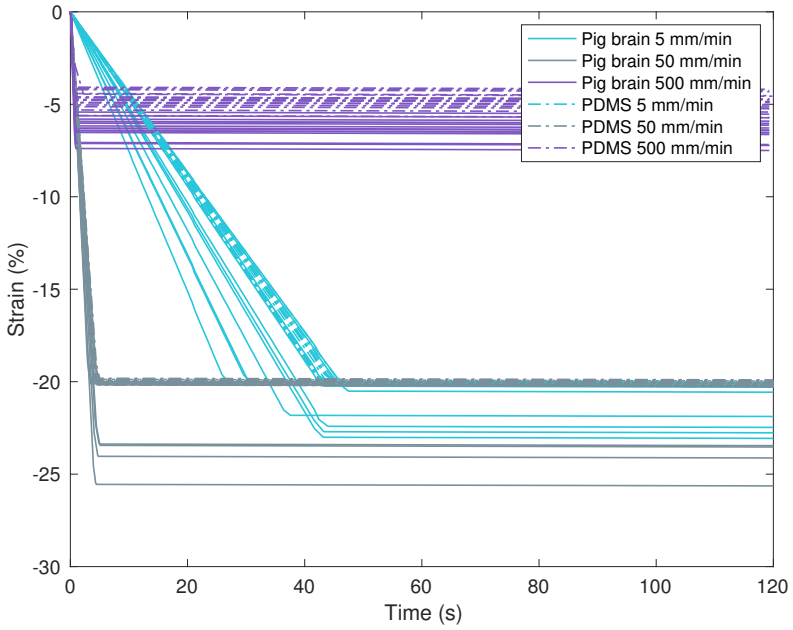

Figure 4: Engineering strain of all pig brains (SWE and NSWE) and PDMS under compression test. Negative strains implies compression of the sample. The entire two minute hold duration is not shown to emphasize the transition from the ramp to hold step.

The stress relaxation results, for linear compressive rates of 5 mm/min, 50 mm/min, and 500 mm/min, are shown in figures 5, 6, and 7, respectively. In these figures, pig brains exposed to a shock wave are labeled as "SWE", while no shock wave exposure is labeled as "NSWE". The stress relaxation behavior of SWE and NSWE pig brains are compared with PDMS of ratio 1:70 and 1:80. Error bars in figures 5, 6, and 7 show the variation in the experimental results. The large error bars in the stress response are attributed to a variety of factors. One factor is that the percentage of white and gray matter in the samples tested varied, even though care was taken

to core samples from the same region of each hemisphere. A comprehensive experimental study on human brains, conducted by Jin et al. (2013), also showed large error bars for engineering stress. Preload also contributed to the variable stress response, even though the preload value did not exceed 0.04 N. The result of PDMS 1:10 is not shown in figures 5 – 7 because PDMS 1:10 is much stiffer than the pig brain. As a result, PDMS 1:10 is excluded to better compare the soft PDMS (1:70 and 1:80) with pig brain. The results using PDMS 1:10 are shown in figure 8. In addition, there is a flat peak in figure 5 because the deviation of peak time exists from the data. The data line shows the average of a set of data; thus, stress from SWE pig brain data shows a small flat region in figure 5.

At linear rates of 5 mm/min (figure 5) and 50 mm/min (figure 6), the stress versus time curves for PDMS and pig brain show a similar trend. When the linear rate increases from 5 mm/min to 50 mm/min, there is an increase in stress for all samples (brain and PDMS). The samples' maximum stress increases with increased linear rate. All pairs of linear rates considered were significantly different and each pair had a $p<0.0001$, for the maximum stress. The average stress of SWE pig brain was lower than the NSWE condition, with the percent difference calculated using the average peak stress at 21% for 5 mm/min and 37% for 50 mm/min. This lower average stress suggests that the brain tissue softens after shock wave exposure, due to neuronal cell damage. The literature has reported that neuronal cell damage (e.g. structural, capillary hemorrhages, and vascular leakages from disruption of the blood brain barrier), following blast exposure, can lead to a softer brain tissue (Kabu et al., 2015; Laksari et al., 2014; Cernak, 2017). Furthermore, our results confirm that the brain is viscoelastic since the stress response is dependent on the linear rate considered. Thus, the linear rate is an important factor to consider when determining a soft tissue's material properties.

The PDMS of ratio 1:70 is significantly different than 1:80 ($p<0.0001$), with an average stress that is 400 Pa higher at low linear rates (5 mm/min and 50 mm/min). The average stress for PDMS with a 1:80 ratio was not significantly different from SWE pig brains ($p=1.0000$). Thus, PDMS with a ratio of 1:80 better captures the mechanical response of SWE brains subjected to stress relaxation, than the 1:70 PDMS ratio compressed to 20% strain.

At the high linear rate (500 mm/min), the average maximum stress for SWE and NSWE pig brain were not statistically different ($p=0.8542$), even though the engineering stress-time curves (figure 7) can be differentiated. When considering only the factor 'All Samples', the average stress for pig

brains exposed to a shock wave five times were significantly different than the pig brains that were not exposed to a shock wave ($p<0.0001$). The stress relaxation curves of PDMS compressed at 500 mm/min are shown in figure 7. The average stress of PDMS with a 1:70 ratio is not statistically different than the NSWE pig brain subjected to stress relaxation tests, at 500 mm/min ($p=1.0000$). When the ratio of PDMS increases from 1:70 to 1:80, the average stress of PDMS decreases. As a result, the average stress between PDMS 1:70 and 1:80 is statistically different when considering lower compressive rates: 5 mm/min ($p<0.0001$) and 50 mm/min ($p<0.0001$). However, figure 7 shows that PDMS with a ratio of 1:70 and 1:80 are not statistically different, in that they both capture the stress response of brain at 500 mm/min ($p=0.9711$). Thus, PDMS with a ratio that ranges from 1:70 – 1:80 can be a potential brain surrogate material for pig brain tissue subjected to high compressive rate loading.

Figure 8 compares PDMS of ratio 1:10, 1:70, and 1:80 at the 500 mm/min linear rate. At 500 mm/min, the maximum strain that the PDMS and brain tissue compressed was $-5\% \pm 2\%$. The 1:10 ratio, which is a suggested ratio for Sylgard 184, shows high stress of about 6×10^4 Pa. Compared to PDMS with a ratio of 1:10, the percent difference for the maximum average engineering stress of PDMS 1:70 and 1:80 is 198.6% and 198.9%, respectively.

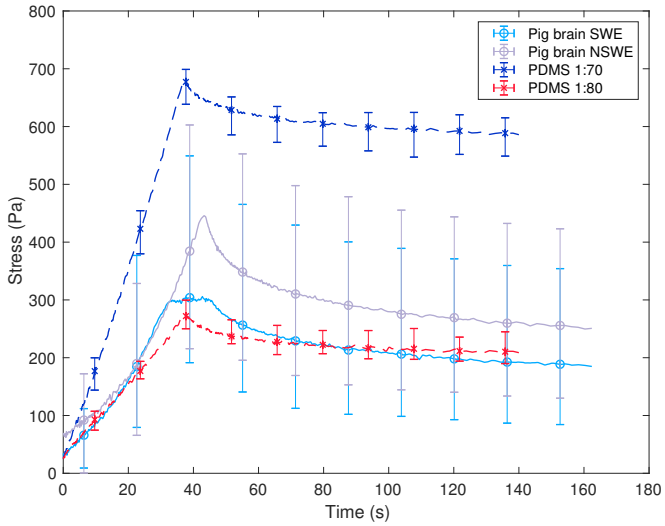

Figure 5: Engineering stress versus time from pig brain in two different conditions (SWE and NSWE) and PDMS of ratio 1:70 and 1:80 at linear rate of 5 mm/min and 20% strain.

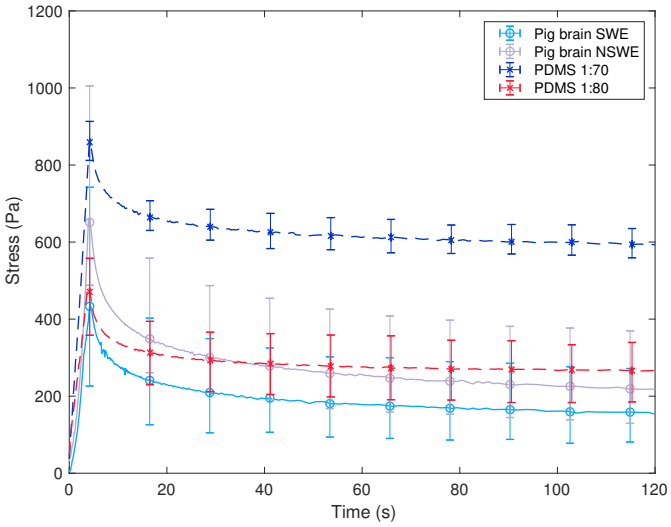

Figure 6: Engineering stress versus time from pig brain in two different conditions (SWE and NSWE) and PDMS of ratio 1:70 and 1:80 at linear rate of 50 mm/min and 20% strain.

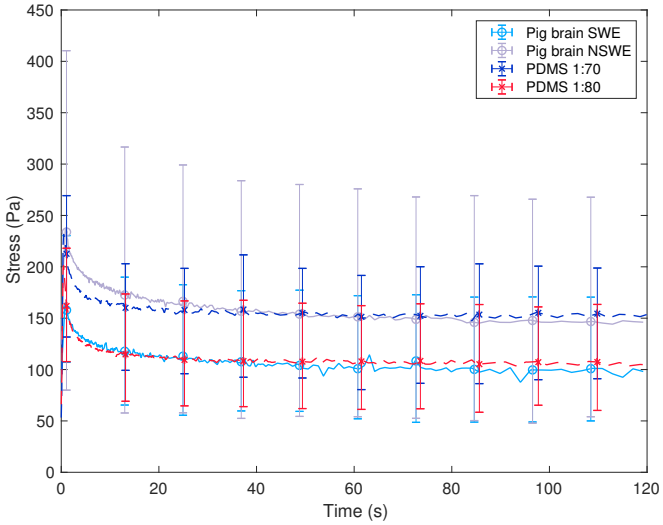

Figure 7: Engineering stress versus time from pig brain in two different conditions (SWE and NSWE) and PDMS of ratio 1:70 and 1:80 at linear rate of 500 mm/min and 5% strain.

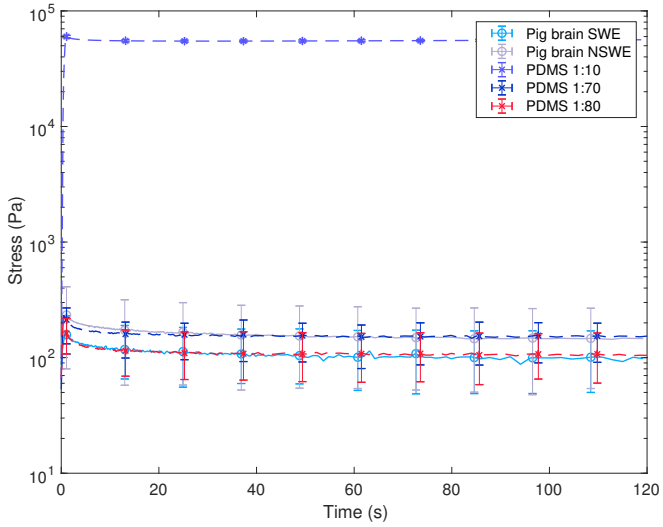

Figure 8: The comparison of engineering stress versus time for PDMS (ratios 1:10, 1:70, and 1:80) and pig brain (SWE and NSWE) at a linear rate of 500 mm/min and 5% strain.

3.2. Curve fit by using Fractional Zener Constitutive Model

An in-house MATLAB (Matlab, 2018) code was developed to optimize the coefficients from the fractional Zener model by fitting the model to the stress relaxation curves from the unconfined compression experiments. The FZ coefficients (E_∞, E_0, τ_0, and α) were obtained for both pig brain and PDMS. Figure 9 shows some examples of the fractional Zener model curve fit for pig brain and PDMS. Due to the large number of experimental data, only representative results are presented. As shown in figure 9, the FZ model was able to capture the pig brain and PDMS stress response from the experimental data. The residuals were used to assess the goodness of fit, and were centered about zero and symmetric.

Due to the preload condition, and variability of the brain specimen, not all experimental data could be described using the optimized constants of the FZ model. Thus, the sample preparation procedure and preload conditions influenced the optimized FZ coefficient values. The averaged optimized FZ coefficients for pig brain and PDMS results are shown in table 3 and are not unique. Thus, to obtain physically realistic FZ coefficient values, an upper and lower bound was defined in the MATLAB code. Alpha for the pig brain ranged between 0.6 – 0.63, which shows that the pig brain behaves more like a Newtonian fluid than an elastic solid. The PDMS with ratio 1:70 and 1:80 had an α between 0.6 – 0.65. The alpha values selected for the brain are in a similar range as those by Bentil and Dupaix (2014) and Davis et al. (2006) of 0.624 and 0.641, respectively. Thus, PDMS exhibits a behavior that is also closer to a fluid when subjected to stress relaxation during an unconfined compression experiment.

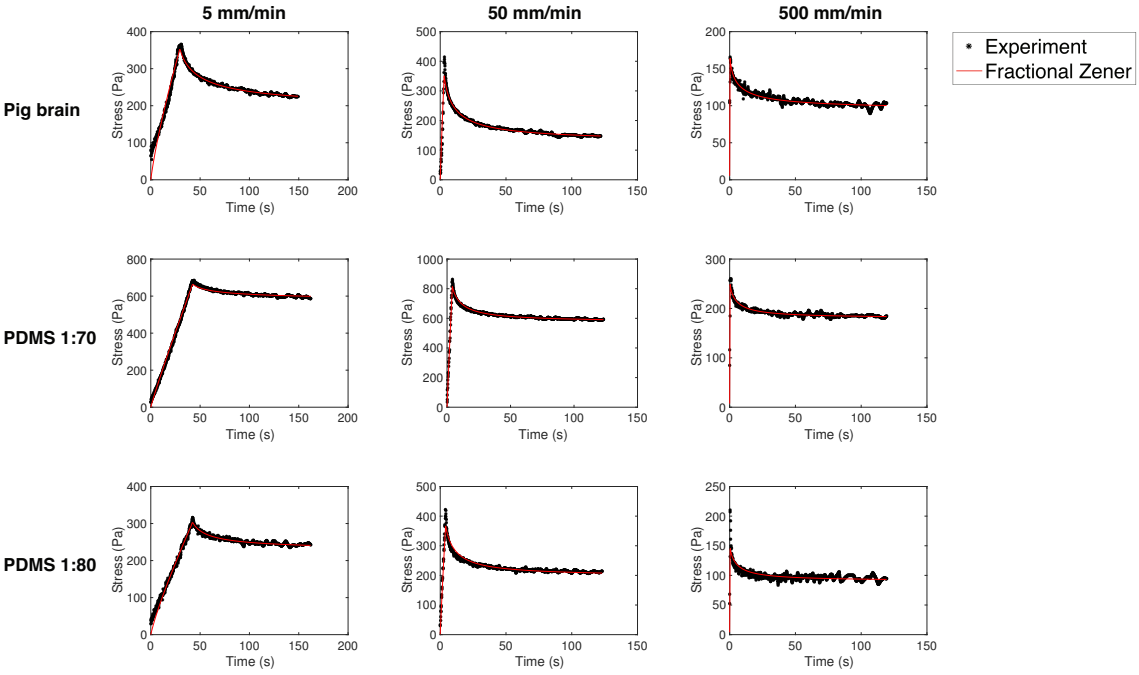

Figure 9: Some examples of the fractional Zener model curve fit for brain and PDMS experimental data at 5 mm/min (20% strain), 50 mm/min (20% strain), and 500 mm/min (5% strain).

Table 3: Coefficients from Fractional Zener Model Curve Fit.

Sample	Sample Size	Condition	Linear rate (mm/min)	E_∞ (Pa)	E_0 (Pa)	τ_0 (s)	α	Alpha Standard Deviation
Pig brain	4	NSWE	5	1013.0	3640.8	7.39	0.60	6.3e-3
Pig brain	4	NSWE	50	756.8	3451.4	7.37	0.61	2.4e-2
Pig brain	8	NSWE	500	6390.7	11176.2	7.46	0.61	1.6e-2
Pig brain	6	SWE	5	770.6	3127.1	7.41	0.60	2e-4
Pig brain	6	SWE	50	633.1	2618.2	7.48	0.62	2.3e-2
Pig brain	8	SWE	500	4078.2	7547.7	7.39	0.62	2.3e-2
PDMS	8	1:70	5	2886.7	4286.2	7.35	0.60	3e-5
PDMS	8	1:70	50	2982.4	4964.2	7.00	0.65	2e-4
PDMS	8	1:70	500	6484.3	9281.1	7.00	0.65	8e-4
PDMS	8	1:80	5	967.3	2381.6	7.12	0.63	1.7e-2
PDMS	12	1:80	50	1269.1	2849.6	7.00	0.65	1.8e-6
PDMS	12	1:80	500	4645.8	7603.9	7.00	0.65	9.1e-3

From table 3, and figures 10 and 11, the changing trend of the coefficients describing the instantaneous modulus or initial elastic response (E_0) and long-term stiffness (E_∞) is shown. From all cases of pig brain and PDMS, the relaxation time coefficient τ_0 is in the range 7 – 7.5 s.

3.3. Statistical Analysis

The discrete factor effects model that yielded the best-fit for each of the response variables (i.e. E_∞, E_0, τ_0, α, and σ_{max}) included 'All Samples', 'Compression Rate', and the binary interaction between 'All Samples' and 'Compression Rate'. P-values from the ANOVA study are provided in table 4. The factors 'All Samples' and 'Compression Rate' were statistically significant, at a significance level of 0.05, despite the large statistical variations in the data. However, the binary interaction of 'All Samples' and 'Compression Rate' was not statistically significant for E_∞ and E_0. As a result, p-values are not reported in figures 10 and 11.

The Tukey HSD test showed that both E_∞ and E_0 are significantly different between 5 mm/min and 500 mm/min ($p<0.0001$), and also 50 mm/min and 500 mm/min ($p<0.0001$). The long-term (E_∞) and instantaneous elastic (E_0) response are not significantly different between the pair 5 mm/min and 50 mm/min, $p=0.9512$ and $p=0.6310$, respectively. Comparing PDMS with ratio 1:70 and 1:80, PDMS 1:80 shows closer FZ averaged coefficient values for E_∞ and E_0 when compared with the pig brain (table 3). For the long-term elastic modulus E_∞, the Turkey HSD test showed that PDMS 1:80 was significantly different than PDMS 1:70 ($p=0.0001$), but was not significantly different from pig brain SWE ($p=0.5758$) and pig brain NSWE ($p=0.8883$). The instantaneous elastic modulus E_0 also showed that PDMS 1:80 was significantly different than PDMS 1:70 ($p=0.0076$), and was not significantly different from pig brain SWE ($p=0.9972$) and pig brain NSWE ($p=0.1244$). These results, using the FZ coefficients, show that the PDMS ratio needed for pig brain surrogates ranges between 1:70 – 1:80. Additionally, the results show that the PDMS ratio selected for the brain surrogate depends on the compressive loading rate of interest.

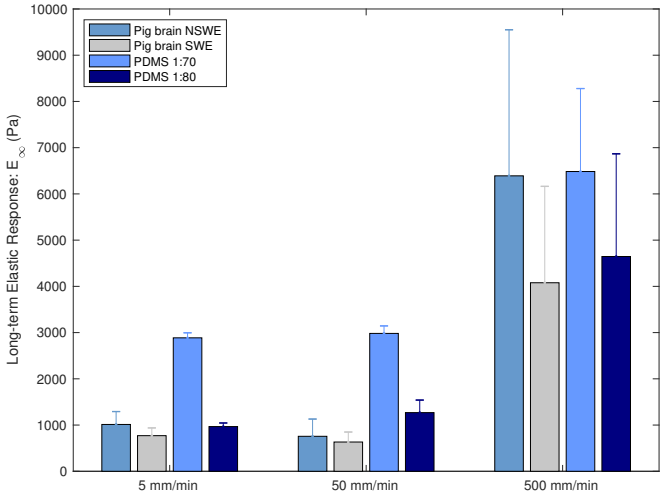

Figure 10: Comparison of the long-term elastic response E_∞ from the FZ model, for pig brain and PDMS at different linear rates.

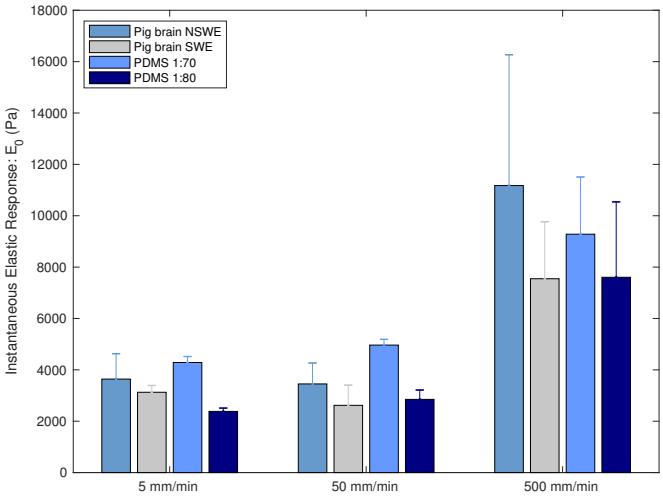

Figure 11: Comparison of the instantaneous elastic response E_0 from the FZ model, for pig brain and PDMS at different linear rates.

Table 4: P-values for the fractional Zener model coefficients and maximum stress (σ_{max}). A p-value less than 0.05 is statistically significant. The binary interaction between the factors 'All Samples' and 'Compression Rate' is denoted by an asterisk (*).

Factor	E_∞ (Pa)	E_0 (Pa)	τ_0 (s)	α	σ_{max} (Pa)
All Samples	< 0.0001	0.0020	< 0.0001	< 0.0001	< 0.0001
Compression Rate	< 0.0001	< 0.0001	< 0.0001	< 0.0001	< 0.0001
All Samples*Compression Rate	0.3772	0.2827	0.0002	0.0003	< 0.0001

4. Discussion and Conclusion

To find a surrogate brain material with properties similar to a brain exposed and unexposed to shock waves, the PDMS (Sylgard 184) ratio was varied and subjected to unconfined compression experiments using the HR-2 rheometer. A linear rate of 5 mm/min, 50 mm/min, and 500 mm/min is applied to both brain and PDMS samples. Sylgard 184 was chosen in this study because it is a common and popular biomaterial with applications in soft tissue prosthesis and surrogates (e.g. brain, artery, muscle, and skin) (Bentil et al., 2016; Abbasi et al., 2001). In addition, PDMS is cheap and easy to fabricate. Future experiments will consider other silicone chemistries (e.g. peroxide or acetoxy cure system). Additionally, PDMS samples will be exposed to shock waves in future studies investigating the material's softening behavior. When making PDMS, the samples were pigmented white with titanium dioxide. The pigment did not significantly affect the elastic properties of PDMS according to Bentil et al. (2016). Pigmenting was conducted for future PDMS study with digital image correlation (DIC). The pigmented PDMS will generate high contrast images for DIC experiments to study the sample's radial expansion.

The stress relaxation results were compared to evaluate if PDMS of ratio 1:70 and 1:80 could be a brain surrogate for experiments investigating bTBI mechanisms. The results show that PDMS with a 1:80 ratio behaved similarly to pig brains. However, at a high linear rate (500 mm/min), both PDMS with a ratio of 1:80 and 1:70 showed similar stress behavior as a pig brain. Thus, after shock wave exposure, the linear rate of compressive load is relatively high. This implies that PDMS with a ratio ranging from 1:70 – 1:80 could be utilized as a brain surrogate during experiments where dynamic compressive loads are applied.

The average stress curve for the pig brain SWE and NSWE could be differentiated for the three linear rates considered. The fractional Zener viscoelastic model was applied to the experimental data. From the FZ curve fit, coefficients were optimized for PDMS and pig brain samples under the aforementioned range of linear rates. FZ coefficients of the elastic modulus (E_∞ and E_0) showed that the stiffness of pig brain samples decrease following shock wave exposure. Coefficients describing the elastic modulus from PDMS and pig brain samples showed an increasing trend with increased linear rates. Optimized coefficients from the FZ model facilitated a comparison of the brain and PDMS material. Results from the curve fit of the FZ model and experimental data shows that PDMS 1:80 has a very similar alpha coefficient when compared with pig brain SWE (p=1.0000).

Previous study by Bentil (2013) and Davis et al. (2006) also considered the fractional Zener model to characterize the brain's material response. From Bentil (2013), pig brain tissue samples were tested at a strain level of 10%, compressive rate of 1 mm/min and 5 mm/min, and FZ coefficient values of $E_\infty = 442$ Pa, $E_0 = 3520$ Pa, $\tau_0 = 7.62$ s, $\alpha = 0.624$. In addition, from Davis et al. (2006) study, the FZ coefficient values for human brain was $E_\infty = 1612$ Pa, $E_0 = 7715$ Pa, $\tau_0 = 6.709$ s, and $\alpha = 0.641$. The percent difference for the long-term elastic modulus (E_∞), using the value found by Bentil (2013) and Davis et al. (2006) was 113.9%. However the percent difference for the brain samples from our work (NSWE) with Bentil (2013) and Davis et al. (2006) was 78.5% and 45.6%, respectively. For the instantaneous elastic modulus (E_0), the percent difference compared with Bentil (2013) and Davis et al. (2006) was 3.4% and 71.8%. Compared with the long-term elastic modulus, the coefficient E_0 for the NSWE brain is close to the result reported by Bentil (2013). The percent difference for τ_0 was 3.1% and 9.7%, which is relatively low. The consistency of relaxation time showed that the initial decay of the stress response is very similar among all the brain samples. For α, similarly, the percent difference was 3.9% and 6.6%, which meant that from the FZ curve fitting, α is quite consistent. Variability in the reported values for the elastic modulus from our work, and Bentil (2013) and Davis et al. (2006), are attributed to factors such as the percentage of gray and white matter in the cored specimen, the diameter of the brain specimen tested, and the strain level considered. For instance, Bentil (2013) conducted experiments using a 15-mm diameter brain to a strain of 10%.

In a recent study by Budday et al. (2017), human brain properties was studied by using a family of finite viscoelastic Ogden-type models. Even

though this model was different from the FZ model, due to the lack of a fractional element, similarities could be made using the instantaneous (μ_1) /long-term modulus (μ_∞) and relaxation time (τ_1). Budday et al. (2017) found that the stiffnesses and time constants were μ_∞=0.7 kPa, μ_1=2.0 kPa, and τ_1=9.7 s in the gray matter cortex and μ_∞=0.3 kPa, μ_1=0.9 kPa, and τ_1=14.9 s in the white matter corona radiata. In another study that applied a first-order Ogden model to study the compression behavior of spinal cord white matter by Sparrey and Keaveny (2011), their results showed that strain rate, preload, and peak strain all significantly affect the stiffness constant μ_1. The same trend that the stiffness constant increased with linear rate has been found in our study. Under a strain rate of 0.005 s^{-1}, Sparrey and Keaveny (2011) found $\mu_1 = 172 \pm 130$ Pa, which is lower than the stiffness results from our results (5 mm/min compressive rate) and Budday et al. (2017).

Van Sligtenhorst et al. (2006) studied compressive properties of bovine muscle tissue in a range of high linear rates. Similar to the soft brain and PDMS (1:70 and 1:80) material, the instantaneous elastic modulus for the muscle tissue also increased with strain rate. From a study on porcine brains conducted by Rashid et al. (2012), they also found that the elastic moduli increased with strain rate. The increased elastic moduli with strain rate was confirmed from our study. Both E_∞ and E_0 FZ coefficients increased when the linear rate was increased from 5 mm/min to 500 mm/min.

Acknowledgements

This research was financially supported by the Roy J. Carver Charitable Trust under Grant #18-5021 and is acknowledged gratefully. The research is also financially supported by Iowa State University through start-up funds to S.A. Bentil, for which the authors are grateful.

References

Abbasi, F., Mirzadeh, H., Katbab, A., November 2001. Modification of polysiloxane polymers for biomedical applications: a review. Polymer International 50 (12).

Alley, M. D., Schimizze, B. R., Son, S. F., January 2011. Experimental modeling of explosive blast-related traumatic brain injuries. NeuroImage 54, S45–S54.

Axelsson, H., Hjelmqvist, H., Medin, A., Persson, J. K., Suneson, A., February 2000. Physiological changes in pigs exposed to a blast wave from a detonating high-explosive charge. Mil Med 165 (2), 119–126.

Bauman, R. A., Ling, G., Tong, L., Januszkiewicz, A., Agoston, D., Delanerolle, N., Kim, Y., Ritzel, D., Bell, R., Ecklund, J., Armonda, R., Bandak, F., Parks, S., June 2009. An introductory characterization of a combat-casualty-care relevant swine model of closed head injury resulting from exposure to explosive blast. J. Neurotrauma 26 (6), 841–860.

Bentil, S., Ramesh, K., Nguyen, T., 2016. A Dynamic Inflation Test for Soft Materials. Experimental Mechanics 56 (5), 759.

Bentil, S. A., 2013. A fractional zener constitutive model to describe the degradation of swine cerebrum with validation from experimental data and predictions using finite element analysis. Doctoral dissertation, The Ohio State University.

Bentil, S. A., Dupaix, R. B., February 2014. Exploring the mechanical behavior of degrading swine neural tissue at low strain rates via the fractional zener constitutive model. J Mech Behav Biomed Mater 30, 83–90.

Bentil, S. A., Dupaix, R. B., 2018. Simulations of hydrogel-coated neural microelectrodes to assess biocompatibility improvement using strain as a metric for micromotion. Biomedical Physics & Engineering Express 4 (3), 035036.
URL `http://stacks.iop.org/2057-1976/4/i=3/a=035036`

Budday, S., Sommer, G., Haybaeck, J., Steinmann, P., Holzapfel, G. A., Kuhl, E., September 2017. Rheological characterization of human brain

tissue. Acta Biomaterialia 60 (15), 315–329.
URL http://www.sciencedirect.com/science/article/pii/S1742706117303884

Carmichael, B., Babahosseini, H., Mahmoodi, S. N., Agah, M., May 2015. The fractional viscoelastic response of human breast tissue cells. Phys Biol 12 (4), 046001.

Cernak, I., Jun. 2017. Understanding blast-induced neurotrauma: how far have we come? Concussion 2 (3), CNC42.
URL https://www.futuremedicine.com/doi/full/10.2217/cnc-2017-0006

Chanda, A., July 2018. Biomechanical modeling of human skin tissue surrogates. Biomimetics 3 (3), 18.

Chanda, A., Callaway, C., Clifton, C., Unnikrishnan, V., September 2016. Biofidelic human brain tissue surrogates. Mechanics of Advanced Materials and Structures, 1–7.

Clemedson, C.-J., April 1956. Shock wave transmission to the central nervous system. Acta Physiologica Scandinavica 37 (2), 204–214.

Clemedson, C. J., Hultman, H., Gronberg, B., October 1953. Respiration and pulmonary gas exchange in blast injury. J Appl Physiol 6 (4), 213–220.

Clemedson, C. J., Hultman, H. I., June 1954. Air embolism and the cause of death in blast injury. Mil Surg 114 (6), 424–437.

Corning, D., 2018. Sylgard 184 silicone elastomer data sheet.
URL https://consumer.dow.com/content/dam/dcc/documents/en-us/productdatasheet/11/11-31/11-3184-sylgard-184-elastomer.pdf?iframe=true

Courtney, E., Courtney, A., Courtney, M., Feb. 2015. A $55 Shock Tube for Simulated Blast Waves. arXiv e-prints 1502, arXiv:1502.06112.
URL http://adsabs.harvard.edu/abs/2015arXiv150206112C

Craiem, D., Magin, R. L., January 2010. Fractional order models of viscoelasticity as an alternative in the analysis of red blood cell (RBC) membrane mechanics. Phys Biol 7 (1), 13001.

Davis, G. B., Kohandel, M., Sivaloganathan, S., Tenti, G., June 2006. The constitutive properties of the brain paraenchyma part 2. fractional derivative approach. Medical Engineering & Physics 28 (5), 455–459.

Ghajari, M., Hellyer, P. J., Sharp, D. J., Feb. 2017. Computational modelling of traumatic brain injury predicts the location of chronic traumatic encephalopathy pathology. Brain 140 (2), 333–343.
URL https://academic.oup.com/brain/article/140/2/333/2770746/Computational-model

Gu, M., Kawoos, U., McCarron, R., Chavko, M., 2017. Protection against Blast-Induced Traumatic Brain Injury by Increase in Brain Volume.
URL https://www.hindawi.com/journals/bmri/2017/2075463/

Holzapfel, G. A., Gasser, T. C., May 2001. A viscoelastic model for fiber-reinforced composites at finite strains: Continuum basis, computational aspects and applications. Computer Methods in Applied Mechanics and Engineering 190 (34), 4379–4403.

Holzapfel, G. A., Simo, J. C., August 1996. A new viscoelastic constitutive model for continuous media at finite thermomechanical changes. International Journal of Solids and Structures 33 (20), 3019–3034.

Hossain, S. G. M., 2010. Material modeling and analysis for the development of a realistic blast headform. Mechanical (and Materials) Engineering – Dissertations, Theses, and Student Research.

Hua, Y., Akula, P., Gu, L., Berg, J., Nelson, C. A., February 2014. Experimental and numerical investigation of the mechanism of blast wave transmission rough a surrogate head. Journal of Computational and Nonlinear Dynamics 9 (3), 031010.

Iwaskiw, A. S., Ott, K. A., Armiger, R. S., Wickwire, A. C., Alphonse, V. D., Voo, L. M., Carneal, C. M., Merkle, A. C., Jan. 2018. The measurement of intracranial pressure and brain displacement due to short-duration dynamic overpressure loading. Shock Waves 28 (1), 63–83.
URL https://doi.org/10.1007/s00193-017-0759-z

Jin, X., Zhu, F., Mao, H., Shen, M., Yang, K. H., November 2013. A comprehensive experimental study on material properties of human brain tissue. Journal of Biomechanics 46 (16), 2795–2801.

JMP, 2015. JMP.

Kabu, S., Jaffer, H., Petro, M., Dudzinski, D., Stewart, D., Courtney, A., Courtney, M., Labhasetwar, V., May 2015. Blast-Associated Shock Waves Result in Increased Brain Vascular Leakage and Elevated ROS Levels in a Rat Model of Traumatic Brain Injury. PLOS ONE 10 (5), e0127971. URL https://journals.plos.org/plosone/article?id=10.1371/journal.pone.0127971

Kohandel, M., Sivaloganathan, S., Tenti, G., Darvish, K., June 2005. Frequency dependence of complex moduli of brain tissue using a fractional zener model. Physics in Medicine and Biology 50 (12), 2799–2805.

Lai, D., Yakimets, I., Guigon, M., September 2005. A non-linear viscoelastic model developed for semi-crystalline polymer deformed at small strains with loading and unloading paths. Materials Science and Engineering: A 405 (1), 266–271.

Laksari, K., Sadeghipour, K., Darvish, K., Apr. 2014. Mechanical response of brain tissue under blast loading. Journal of the Mechanical Behavior of Biomedical Materials 32, 132–144. URL http://www.sciencedirect.com/science/article/pii/S1751616113004323

Lu, T., Wang, J., Yang, R., Wang, T., November 2016. A constitutive model for soft materials incorporating viscoelasticity and mullins effect. Journal of Applied Mechanics 84.

Mainardi, F., 2010. Fractional Calculus and Waves in Linear Viscoelasticity: An Introduction to Mathematical Models. World Scientific.

Masoumi, N., Framanzad, F., Zamanian, B., Seddighi, A. S., Moosavi, M. H., Najarian, S., Bastani, D., 2013. 2d computational fluid dynamic modeling of human ventricle system based on fluid-solid interaction and pulsatile flow. Basic Clin Neurosci 4 (1), 64–75.

Matlab, 2018. Matlab 2018a. The MathWorks Inc.

Mediavilla Varas, J., Philippens, M., Meijer, S. R., van den Berg, A. C., Sibma, P. C., van Bree, J. L. M. J., de Vries, D. V. W. M., September 2011. Physics of IED blast shock tube simulations for mTBI research. Front Neurol 2.

Miller, K., May 1999. Constitutive model of brain tissue suitable for finite element analysis of surgical procedures. Journal of Biomechanics 32 (5), 531–537.

Miller, K., Chinzei, K., April 2002. Mechanical properties of brain tissue in tension. Journal of Biomechanics 35 (4), 483–490.

Miquelard-Garnier, G., Croll, A. B., Davis, C. S., Crosby, A. J., 2010. Contact-line mechanics for pattern control. Soft Matter 6 (22), 5789.

Nakagawa, A., Manley, G. T., Gean, A. D., Ohtani, K., Armonda, R., Tsukamoto, A., Yamamoto, H., Takayama, K., Tominaga, T., February 2011. Mechanisms of primary blast-induced traumatic brain injury: Insights from shock-wave research. Journal of Neurotraum 28 (6), 1101–1119.

Payne, T., Mitchell, S., Bibb, R., Waters, M., January 2015. The evaluation of new multi-material human soft tissue simulants for sports impact surrogates. Journal of the Mechanical Behavior of Biomedical Materials 41, 336–356.

Ploch, C. C., Mansi, C. S., Jayamohan, J., Kuhl, E., June 2016. Using 3d printing to create personalized brain models for neurosurgical training and preoperative planning. World Neurosurgery 90, 668–674.

Qi, H. J., Boyce, M. C., October 2004. Constitutive model for stretch-induced softening of the stressstretch behavior of elastomeric materials. Journal of the Mechanics and Physics of Solids 52 (10), 2187–2205.

Rashid, B., Destrade, M., Gilchrist, M., June 2012. Mechanical characterization of brain tissue in compression at dynamic strain rates. Journal of the Mechanical Behavior of Biomedical Materials 10, 23–38.

Säljö, A., Arrhén, F., Bolouri, H., Mayorga, M., Hamberger, A., December 2008. Neuropathology and pressure in the pig brain resulting from low-impulse noise exposure. Journal of Neurotrauma 25 (12), 1397–1406.

Schiavone, P., Chassat, F., Boudou, T., Promayon, E., Valdivia, F., Payan, Y., August 2009. In vivo measurement of human brain elasticity using a light aspiration device. Medical Image Analysis 13 (4), 673–678.

Selvan, V., Ganpule, S., Kleinschmit, N., Chandra, N., 2013. Blast wave loading pathways in heterogeneous material systems-experimental and numerical approaches. Journal of Biomechanical Engineering 135 (6), BIO–12–1198.

Sollich, P., July 1998. Rheological constitutive equation for a model of soft glassy materials. Phys. Rev. E 58 (1), 738–759.

Sparrey, C. J., Keaveny, T. M., January 2011. Compression behavior of porcine spinal cord white matter. Journal of Biomechanics 44 (6), 1078–1082.

Supplementary Material (ESI) for Lab on a Chip, 2007. The Royal Society of Chemistry.

Takagi, H., Takahashi, M., Maeda, R., Onishi, Y., Iriye, Y., Iwasaki, T., Hirai, Y., May 2008. Analysis of time dependent polymer deformation based on a viscoelastic model in thermal imprint process. Microelectronic Engineering 85 (5), 902–906.

Van Sligtenhorst, C., Cronin, D. S., Wayne Brodland, G., January 2006. High strain rate compressive properties of bovine muscle tissue determined using a split hopkinson bar apparatu. Journal of Biomechanics 39 (10), 1852–1858.

Wang, Z., Volinsky, A. A., Gallant, N. D., November 2014. Crosslinking effect on polydimethylsiloxane elastic modulus measured by custom-built compression instrument. Journal of Applied Polymer Science 131 (22).

Xu, H., Jiang, X., March 2017. Creep constitutive models for viscoelastic materials based on fractional derivatives. Computers & Mathematics with Applications 73 (6), 1377–1384.